Proceedings of the ASME 2009 28th International Conference on Ocean, Offshore and Arctic Engineering
OMAE2009
May 31 - June 5, 2009, Honolulu, Hawaii, USA

OMAE2009-79717

A TRUSS SEMISUBMERSIBLE OPTIMIZED FOR THE POST KATRINA ENVIRONMENT IN GULF OF MEXICO CORRELATED WITH MODEL TEST

Chan K. Yang
FloaTEC, LLC
Houston, TX 77079, USA
ckyang@floatec.com

John Murray
FloaTEC, LLC
Houston, TX 77079, USA
jmurray@floatec.com

Hanseong Lee
FloaTEC, LLC
Houston, TX 77079, USA
hslee@floatec.com

Myoungkeun Choi
FloaTEC, LLC
Houston, TX 77079, USA
mchoi@floatec.com

Cheng-Yo Chen
J. Ray McDermott Engineering
Houston, TX 77079, USA
CYChen@mcdermott.com

Yun Ding
J. Ray McDermott Engineering
Houston, TX 77079, USA
yyding@mcdermott.com

ABSTRACT

This paper presents a Truss Semisubmersible (Truss Semi) design optimized to meet the post-Katrina Gulf of Mexico (GoM) environment criteria, with global performance correlated in 1:50 scale model tests in a wave basin.

A conventional semisubmersible with a ring pontoon is facilitated with heave plates supported by the truss structure to increase heave natural period. The size of the semisubmersible hull and the configuration of the heave plates are optimized through frequency domain analysis to minimize the vertical motion enough to allow the dry trees to accommodate top tensioned production risers.

The system includes eight production top tension risers (TTRs) connected to the production deck and a single drilling riser connected to the drilling deck. All of the TTRs are connected through the hydro-pneumatic tensioner system. One gas export and one oil export steel catenary riser (SCR) export the oil and gas to the storage facility. Structures designed for this deepwater area (4,300 ft) of the central Gulf of Mexico (GoM) must be designed to meet newly proposed environmental criteria [1].

The optimized Truss Semi was tested in the Offshore Technology Research Center (OTRC) model basin, to confirm the global performance, such as motion, air gap and loads on the heave plates. The numerical predictions correlate well with the model test results.

Key Words : Truss Semisubmersible, post-Katrina Gulf of Mexico (GoM), model test, dry trees, steel catenary risers (SCRs), top tensioned risers (TTRs).

INTRODUCTION

The Truss Semisubmersible comprises a semisubmersible with heave plates attached beneath the hull and supported by the truss structure as shown in Fig.1. The conventional or deep draft semisubmersibles have relatively good rotational motion characteristics, but they have much larger heave motion than the Spar and TLP dry tree platforms in Gulf of Mexico. The reason for the larger heave motion is that the heave natural frequency is within the wave frequency range of extreme environment in the GoM. Several successive hurricanes, including Ivan, Katrina and Rita, showed that the environmental criteria for platform design in the GoM is more exacting than was allowed for in earlier design criteria.

The harsher environmental criteria, which are based on the hindcast of the hurricanes, are also implemented by API, especially for the central region of GoM[1]. Efforts are being made to reassess the global performance of the existing platforms under the Post-Katrina environment[2], and the new designs of the platforms already follow the new criteria and procedures[3][4].

These conditions make the predicted performance of the conventional semisubmersible worse in terms of its motion.

Heave plates can effectively raise the heave added mass to increase the heave natural period. The positive effect of the heave plates on the conventional semisubmersible with twin

pontoons has been addressed with the model test [5]. The heave plates also play a significant role in controlling the wave exciting force. The plates change the first hump of the RAOs at the wave period around ten seconds and the cancellation point, where the wave exciting force becomes zero through the interaction between the hull and the heave plates. The position and size of the heave plates as well as the size of the semisubmersible hull (column, pontoon, and draft) are considered as control parameters to minimize the heave motion. Frequency domain analysis and time domain analysis were used to check the performance during optimization.

The 1:50 scale model tests were carried out with the selected configuration at OTRC in College Station, TX. The twelve mooring lines were lumped into four lines, and the nine top-tensioned risers were lumped into one equivalent riser. The mooring lines were truncated for the test to give equivalent horizontal and vertical stiffness. The hull motion, deck acceleration, mooring tension, air gap, riser tension, riser reaction force at the keel joint, and the connector loads on the truss were measured for 1,000-Year, 100-Year and 10-Year environments. White noise irregular waves were also applied to determine the RAOs. The motion and reaction force RAOs as well as the three-hour extreme values of the measured data were introduced and compared with the numerical predictions.
The time domain simulation was carried out by using the coupled global motion analysis program, HARP/Charm3D [6]. Charm3D is based on the hybrid model of Morison members and a panelized body. The hydrodynamic forces on the column and pontoon were obtained using WAMIT, which uses the potential flow approach. Viscous effects were determined by applying the Morison equation. WAMIT [7] was used to calculate the frequency domain hydrodynamic coefficients such as added mass and damping and the first- and second-order wave excitation forces.
In general, there is good agreement between the model test results and the numerical predictions. The Truss Semi exhibited good motion characteristics that are comparable to Spar platforms.

OPTIMIZING THE TRUSS SEMI

Table 1 shows the payload and the number of risers. Eight production TTRs and one drilling riser with gas/oil export SCRs are attached to the hull. The total payload including the riser top tension is 20,871 short tons. The well bay slots and the sea floor layout are shown in Fig.2. There are three mooring lines consisting of chain-polyester-chain per corner. Fig.3 shows the mooring configuration . Table 2 shows the mooring system properties.
The properties of production TTRs and the drilling riser are shown in Table 3 and Table 4, respectively. A single casing riser of 10.75 in. OD with 0.6 in. wall thickness is used for the production riser, and a single casing riser of 16 in. OD with 0.75 in. thickness is used for drilling. The tensioner stiffness at the zero stroke for the production riser is 14.3 kips/ft. The stiffness of the drilling riser is 25.7 kips/ft.
The hull and heave plate configuration were obtained to assure stability for the intact and damaged conditions and to reduce vertical motion.
Fig.4 shows the parameters that can affect the Truss Semi global motions, which are varied through a range to identify the optimum values.
Fig.5 shows the effect of varying the heave plate width, which has a significant effect on the heave natural period and the corresponding cancellation point. The three-hour maximum heave decreases as the size of the heave plates increases because the larger plate size increases the natural period. There is an optimal point at which the heave motion reaches its minimum because the wave excitation force increases as the heave plate size becomes larger.
Fig.6 shows the heave RAO changes in relation to the change in the size of the heave plate. The natural period increases from 20 seconds to 30 seconds with the change in heave plate size from 115.2 ft to 187.2 ft. However, the first hump in the wave frequency region also becomes slightly larger.
After some optimization, the hull and heave plate size used in the model design are shown in Table 5. Fig. 7 shows the hull configuration.

NUMERICAL MODELING

The time domain analysis is the direct numerical integration of equations of motion allowing the inclusion of all system nonlinearities. Equation (1) describes the equation of motion for the fully coupled nonlinear model of a floating platform.

$$\left[M + M^{a}(\infty)\right]\underline{\ddot{x}} + \left[K + K_C(\underline{x},t)\right]\underline{x} = \underline{F}_I(t) + \underline{F}_R(\underline{\dot{x}},t) + \underline{F}_m(\underline{x},t) + \underline{F}_{wind}(t) + \underline{F}_C(\underline{x},\underline{\dot{x}},\underline{\ddot{x}},t) \quad (1)$$

M : system mass matrix,

K : system stiffness matrix (hydrostatic),

$M^{a}(\infty)$: Equivalent added mass of the body at infinite frequency,

$\underline{F}_I(t) = \underline{F}^{(1)}{}_I(t) + \underline{F}^{(2)}{}_I(t)$: Wave exciting force of the first and the second order,

$\underline{F}_R(\underline{\dot{x}},t) = -\int R(t-\tau)\underline{\dot{x}}d\tau$: radiation damping force,

$R(t) = \frac{2}{\pi}\int_0^{\infty} C(\omega)\frac{\sin\omega t}{\omega}d\omega$: Retardation function from damping coefficient,

$\underline{F}_{wind}(t)$: wind force,

$\underline{F}_m(\underline{x},t)$: force on the Morison members,

K_C : implicit time and motion dependent stiffness matrix coupling tendon dynamics with platform motion,

$\underline{F}_C(\underline{x}, \underline{\dot{x}}, t)$: motion and time dependent force coupling mooring/riser dynamics with platform motion.

Charm3D software uses the elastic rod technique to model the mooring line/riser/tendon system. This model is ideal for small strain, large displacement structural analysis of slender members such as tendons, risers, and catenary mooring lines. This technique uses a single global coordinate system in the finite element formulation of the rod model. The line model is coupled by a linear rotational spring with the hull at the connection point. The interaction between motions of the hull and the line elements are thus simulated. A nonlinear hydro-pneumatic tensioner model is used for the tensioner at the top of the TTRs.

The Fig.8 shows the configuration of a slender rod model and the free body diagram of forces and moments. The position vector $\underline{r}(s,t)$ is a function of the arc length s of the rod and time, t. $\underline{F}$ and $\underline{M}$ are total resultant force and moment, respectively, acting on the rod cross section. The distributed load $\underline{q}$ is divided as follows.

$$\underline{q} = \underline{w} + \underline{F}^s + \underline{F}^d \quad (2)$$

where

$\underline{w}$: weight of the rod per unit length,

$\underline{F}^s$: hydrostatic force on the rod per unit length,

$\underline{F}^d$: hydrodynamic force per unit length.

The hydrodynamic forces are modeled using the Morison approach as shown in Equation 3.

$$\underline{F}^d = -C_A \rho A_I \underline{\ddot{r}}^n + C_M \rho A_I \underline{\dot{V}}^n + C_D \rho A_D \left| \underline{V}^n - \underline{\dot{r}}^n \right| \left(\underline{V}^n - \underline{\dot{r}}^n \right) \quad (3)$$

where $C_M = C_A + 1$: inertia coefficient,

A_I : unit volume of the Morison member for inertia load,

A_D : projected area of the Morison member for drag force,

C_A : added mass coefficient,

C_D : drag coefficient,

ρ : water density,

$\underline{V}^n$: water particle velocity normal to the rod member.

The tension due to the pneumatic tensioner is related with stroke of the piston. Details of the nonlinear model are found in [8]. The Coulomb friction force between the tensioner piston and the cylinder is assumed to be related to the tension [8]. The dynamic friction factor is typically set in the range of 0.02-0.05. A value of 0.025 was selected for this study.

ENVIRONMENTAL CONDITION

Model tests included 10-Year Winter Storm conditions and 100-Year and 1,000-Year hurricane post-Katrina environmental criteria required for the central region of the GoM[1]. Detailed wave, wind and current data are shown in Table 6. The new criteria include a 15.4-second wave peak period for 100-Year hurricane conditions. The new criteria also include higher wave heights, wind speed, and current. The wind, wave and current are assumed to be co-linear. Both 90-degree and 135-degree heading angles are considered. The white noise with the significant wave heights of 20 ft and 40 ft are also applied to determine the wave frequency response of the system and the effect of the wave steepness on motion characteristics.

RESULTS AND DISCUSSION

Table 7 shows the wind area and the center of pressure of the topside and the hull above the MWL at 135-degree and 90-degree wind headings. Table 8 introduces the current load and the corresponding center of pressure at each environmental condition. The dynamic wind loads are applied with a feedback controlled line and winch system to match the wind force. The current loads are applied with the static winch load.

Fig. 9 shows the numerical model of the prototype. The modeled water depth is limited by the depth of the model basin which results in truncated mooring and riser systems. The model of the mooring required the 12 mooring lines to be lumped to one line per corner. The line length was truncated as shown in Fig.10. The nine TTRs were also lumped into one, with the length truncated to fit the pit depth (about 52 ft in model scale) as shown in Fig.11. The truncated mooring and riser systems were verified with a numerical analysis of the model systems in the basin. Results are compared in (Fig.12).

Figure 13 shows the position of the measuring instruments. The six degree of freedom (DOF) motions were measured by an LED system. The accelerations at the deck center were measured using horizontal and vertical accelerometers located at the four corners of the deck. Wave run-up and air gap were measured using the wave probes located at the critical positions. The riser and mooring top tensions were also measured using the single degree of freedom load cell. The six degree of freedom load cell was used to measure the loads between the truss and the semi.

As a result of the static offset test, the horizontal offset and the vertical set-down curves for the 135-degree position are plotted in Fig.14 and Fig.15, respectively. The symbols represent the measured values, the red line shows the predictions based on the model test setup, and the black line shows the results for the prototype. The curves match well within a reasonable range.

Fig.16 compares an example of the surge and heave free decay of model test and the numerical simulation, which provides the natural period and the damping ratio. Table 9 shows the natural period and the damping ratio (% of critical damping) measured, which is compared with the numerical results. Both results show good agreement with 7% error ranges except for the yaw

natural period, which has very little influence on the global performance. The heave natural period is about 25 seconds, which is about 10 seconds away from the 100-Year wave dominant peak period.

White noise (Hs=20ft and 40ft) tests were carried out in the model tests and computed in numerical simulations to obtain the system's RAOs. Results are compared in Fig.17 through Fig.19. The surge RAO in Fig.17 is for a 135-degree heading angle and the response is measured relative to the system's center of gravity (CG).

The roll RAO in Fig.18 shows some discrepancies between the numerical predictions and the model test data. This could be the result of the model's roll response in the of the wave frequency range. The heave RAO shows the smearing phenomenon at the cancellation point due to the viscous effect. This phenomenon is also addressed for the dry tree semisubmersible [9]. The effect becomes larger as the wave steepness increases. As a result, the heave RAO of white noise test with Hs=40 ft has a larger RAO around the cancellation point.

Fig.20 and Fig.21 show the horizontal and the vertical acceleration at the deck center for a 90-degree heading angle. The heave acceleration RAO has similar phenomena to the heave motion RAO around the cancellation point.

The air gap is the relative distance between the bottom of the deck and the water surface. The air gap is affected by vessel motions and relative surface elevation. Both the motions and surface contain frequency components equal to the wave frequencies as well as second-order difference and sum frequencies. The dominant part for the semisubmersible motion occurs at the wave frequencies. Thus, if the surface elevation and the vessel motions are accurately predicted, the air gap can be adequately estimated from numerical methods. The relative motion RAOs on the windward column for a 90-degree heading angle and the RAOs for the leeward column at a 135-degree heading angle are compared in Fig.22 and Fig.23.

The RAOs have a different shape depending on the location measured due to the wave diffraction patterns and the Semi motion. The numerical simulations for surface elevation consider the linear incident and diffraction effects only. Simulations for the 1000-Year hurricane wave dominant conditions are shown in Fig.24 and Fig.25.

The corresponding wave time histories at the front of the leeward column at the 135-degree heading angle and at the windward column for the 90-degree heading angles are shown in Fig.26 and Fig.27, respectively. The dotted line of the upper figure shows the incident waves, and the solid line shows the diffracted waves. The lower figures show the relative motion time history. The leeward elevations have amplified diffracted wave effects with a close phase relationship to the incident waves. The windward side of the column shows elevations closer to the undisturbed incident wave elevations.

Fig.28 and Fig.29 compare the target and measured wave and wind spectrum, respectively, used in the irregular wave tests. The environments are iteratively calibrated.

A snapshot of the irregular wave test with 100-Year hurricane wave dominant condition is shown in Fig.30. The picture in Fig.30 shows a steep breaking wave and it also shows a positive air gap.

The results of the irregular wave tests for both 90 and 135 degree heading angle are plotted in Fig.31 through Fig.36. The maxima shown in the figures are determined from Weibul distributions generated from three-hour simulations. A similar method was used to determine the minima. The range is determined by adding the magnitudes of the respective maxima and minima.

The measured values of the offset shown in Fig.31 are approximately 10% smaller than the calculated values. This is because the mean offset in the computed values includes the loads on the moorings and risers. These were not accurately modeled in the tests. The maximum offset for the 100- Year hurricane wind dominant is simulated to be 6% and measured to be 5.4% due to this mean offset difference (See Fig.32). The heave motion ranges which have a significant effect on the dynamic stroke of the tensioner are plotted in Fig.33. The maximum range for 100-Year hurricane wave dominant case is measured at 17ft and predicted at 16.5ft. In Fig.34, the maximum heel angle is plotted and the measured values. The predicted results have a consistent difference because the heeling moment of the truncated model is not the same as that of the prototype and cause a large mean heel angle (maximum 2 degrees). The measured heel angle for 100-Year hurricane is 8.7 degrees which is almost identical to the numerical prediction. The motions are very similar to the dry tree Spar motion based on the reassessment results for the post-Katrina environmental reported in [2].

Fig.34 shows a difference in the horizontal acceleration. This is due to the difference in mean heel angle that changes the gravitational acceleration components. The horizontal acceleration for 100-Year wave dominant environment is measured to be 0.3×g and calculated to be 0.23×g. As shown in Fig.35, the vertical accelerations correlate very well with the numerical simulation which can be expected from the wave frequency RAOs. The effect of the low frequency is very small.

The minimum air gaps are shown in Fig.36 for the design conditions only. The short and the long wave for 1000 -Year wind and wave dominant cases are considered to be sensitivity cases and were excluded from the air gap calculation. It is seen that minimum air gap is positive for 1000 -Year condition and is about 5 ft for 100 year conditions.

SUMMARY AND CONCLUSION

The Truss Semi with three heave plates is optimized for the central GoM environment with a 4,300ft water depth. The topsides include a drilling rig for the work-over, and dry trees which require the low motion characteristics as compared with a traditional wet tree semisubmersibles. The model tests were carried out with this optimized design and the results show very good agreement with the numerical simulations.

The Truss Semi motions are very close to a dry tree Spar in a similar environment, and the concept has the main advantage of quayside installation and integration.

ACKNOWLEDGMENTS

The authors would like to thank J. Ray McDermott and FloaTEC, LLC for support in preparing the paper.

REFERENCES

[1] API, 2007, “Interim Guidance on Hurricane Conditions in the Gulf of Mexico”, Bulletin 2INT-MET.

[2] John Murray, Chan K. Yang, Hanseung Lee, Wooseuk Yang and Apurva Gupta, “Sensitivity Analysis of Deepwater Floaters to New Gulf of Mexico Metocean Criteria”, DOT 2008 in Houston.

[3] John Murray, Chan K. Yang, Wooseuk Yang, Partha Krishnaswamy, and Jun Zou, 2008, “An Extended Tension Leg Platform Design for Post-Katrina Gulf of Mexico”, Proceedings of ISOPE 2008 in Canada.

[4] John Murray, Chan K. Yang, Cheng-Yo Chen and Edwin Nah, “Two Dry Tree Semisubmersible Designs for Ultra Deep Water Post-Katrina Gulf of Mexico”, Proceedings of OMAE 2008 in Estoril, Portugal.

[5] Cheng-Yo Chen, John Murray, Trevor Mills and Yun Ding, 2008, “Improving the Motions of a Semi by the Addition of Heave Plates”, Proceedings of OMAE in Portugal, OMAE2008-57135.

[6] M.H. Kim, “WINPOST 3.5 Manual”, OTRC Texas A&M University.

[7] Lee, C.H., 1995, “WAMIT Theory Manual”, Department of Ocean Engineering, MIT, MA.

[8] Chan K. Yang, Arcandra Tahar and M.H. Kim, 2007, “Linear and Nonlinear Approach of Hydro-Pneumatic Tensioner Modeling for Spar Global Performance”, Proceedings of OMAE ’07 in California.

[9] John Murray, Arcandra Tahar, and Chan K. Yang, 2006, “Hydrodynamics of Dry Tree Semisubmersibles “, Proceedings of ISOPE-2275 in Lisbon, Portugal.

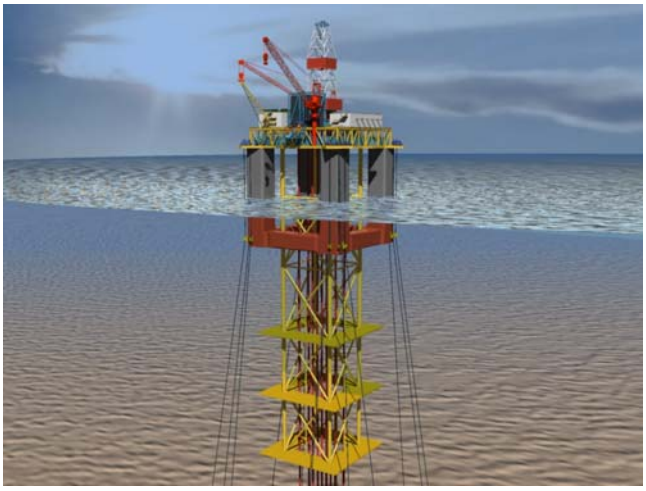

Fig.1 A Configuration of Truss Semi with Three Heave Plates

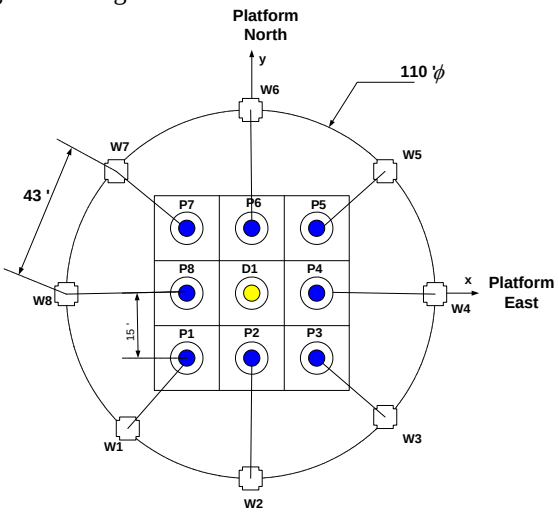

Fig.2 Sea Bed and Well Bay Layout of the Eight Production and One Drilling TTRs

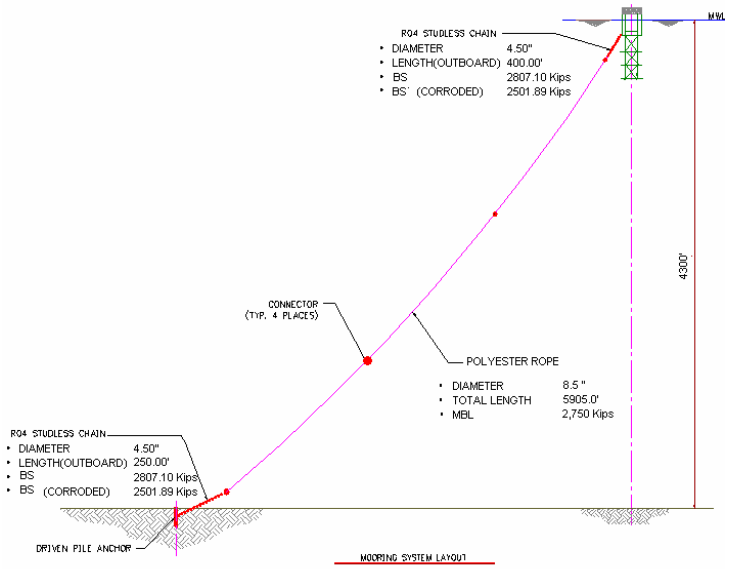

Fig.3 Configuration of Mooring Line – Elevation View

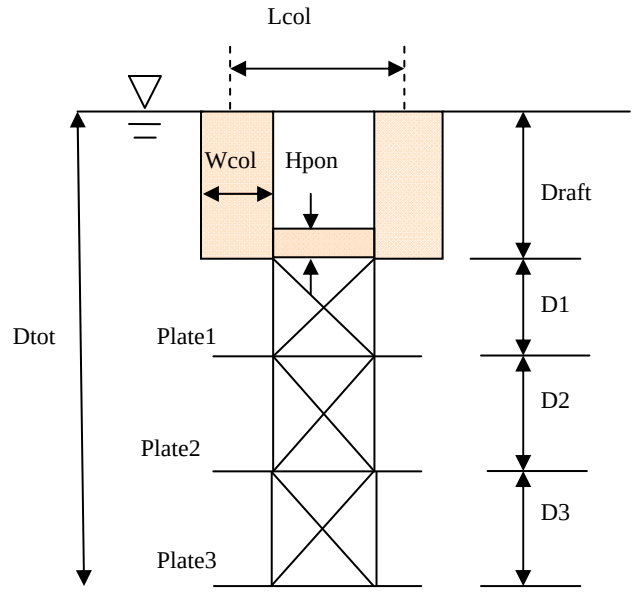

Fig.4 Parameters of Truss Semi with Three Heave Plate

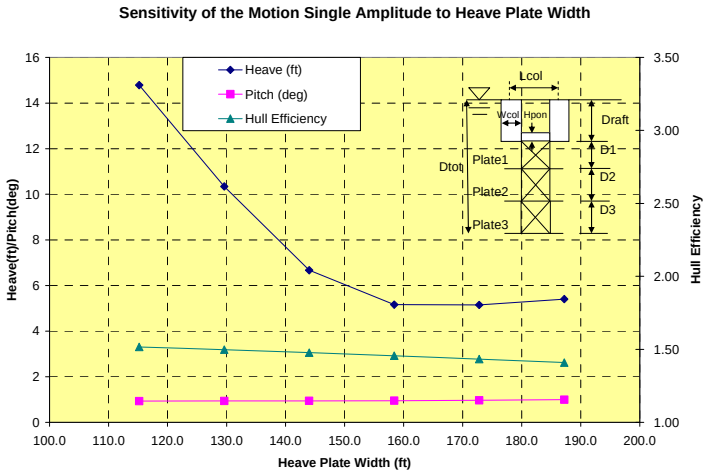

Fig.5 Sensitivity of the Motion Single Amplitude to the Heave Plate Width

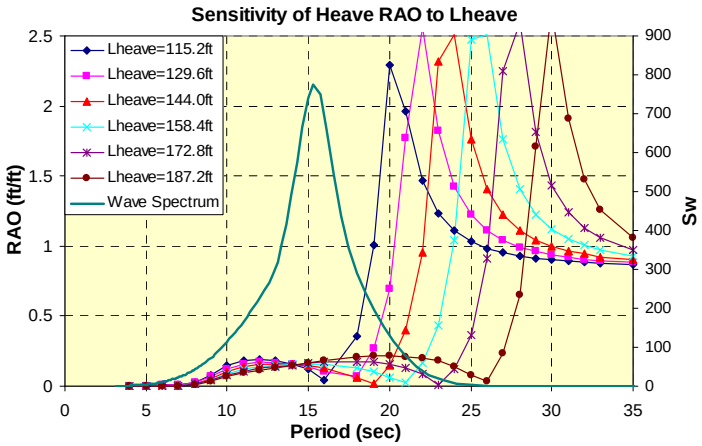

Fig.6 The Sensitivity of Heave RAOs to the Heave Plate Width

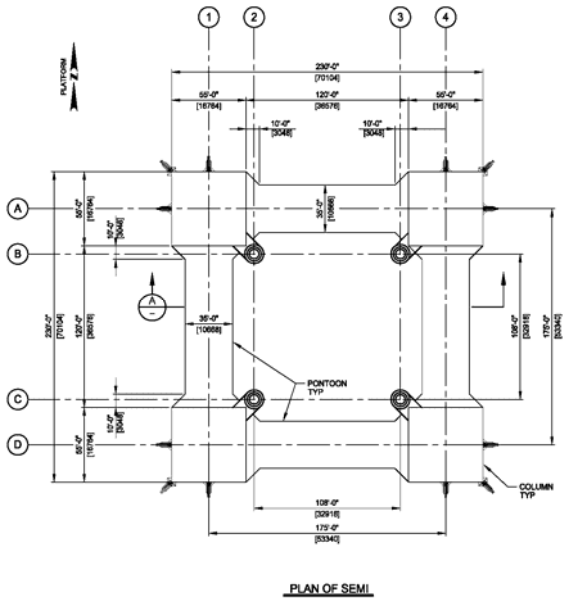

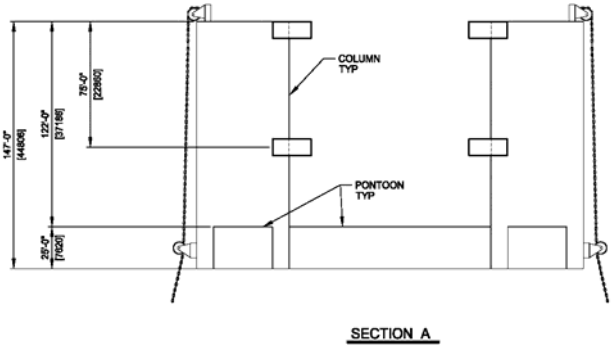

Fig.7 Hull Configuration

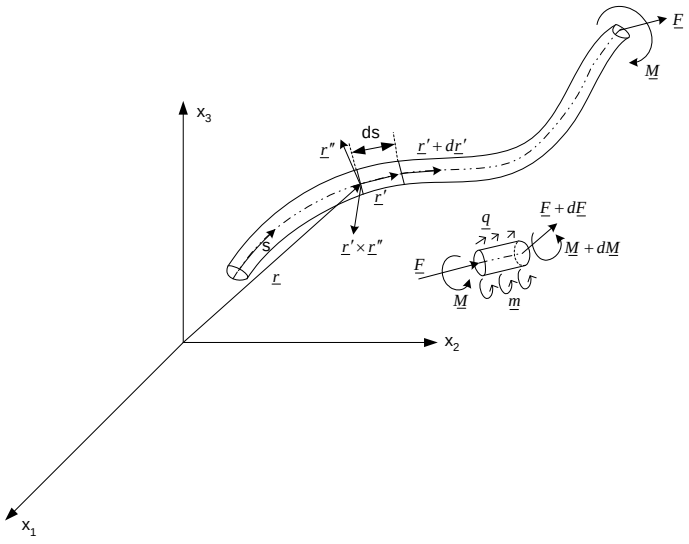

Fig.8 Configuration of Slender Rod Model and Free Body Diagram of Forces and Moments

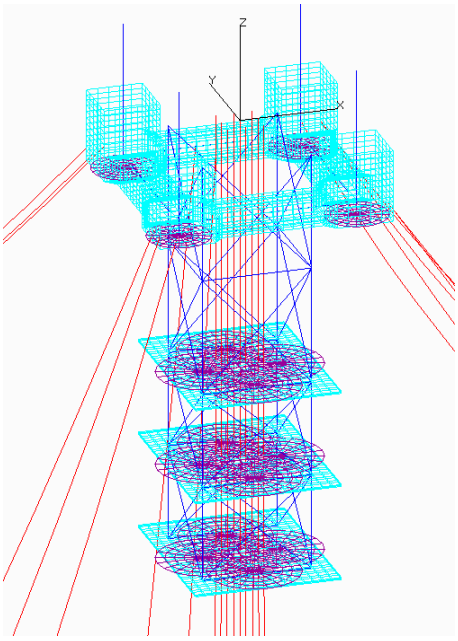

Fig.9 Fully Coupled Model with Morison Members

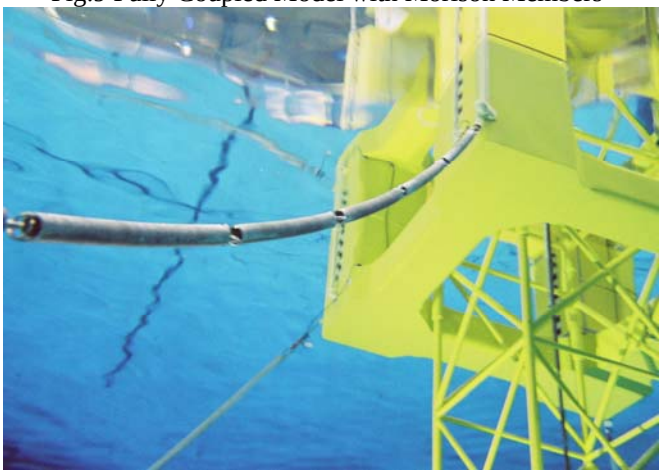

Fig.10 Under-water View of Lumped and Truncated Mooring Line

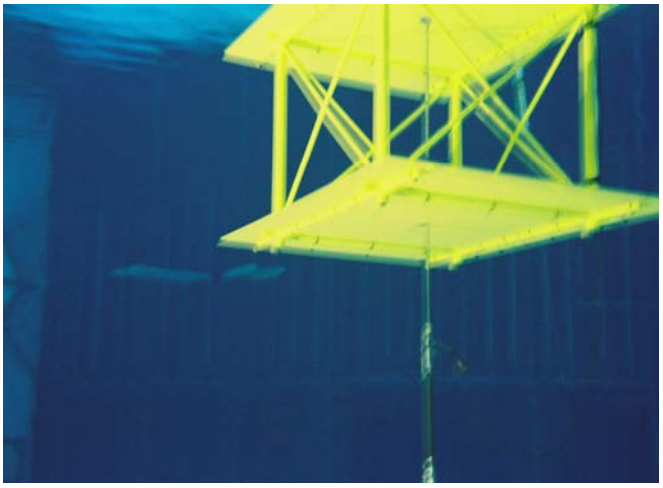

Fig.11 Under-water View of Lumped and Truncated TTR

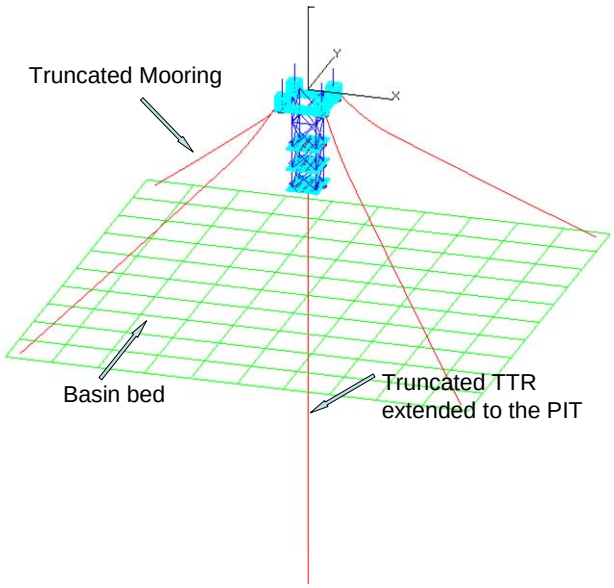

Fig.12 Under-water View of Lumped and Truncated TTR

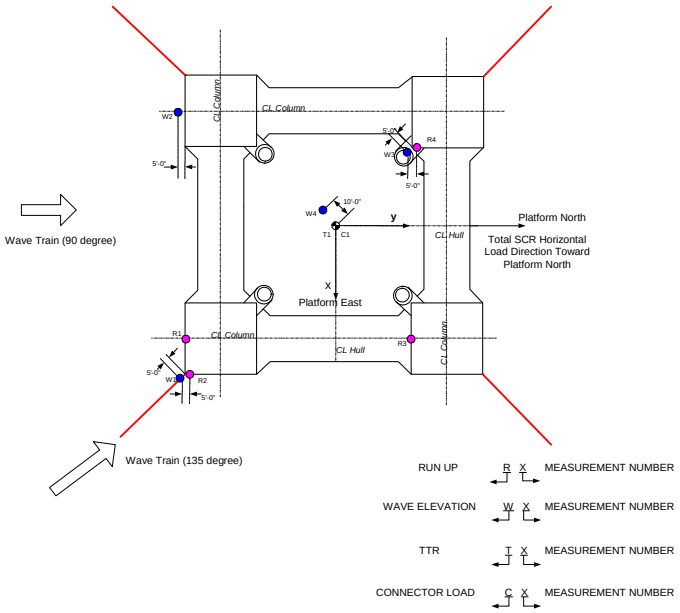

Fig.13 Location of the Measurement

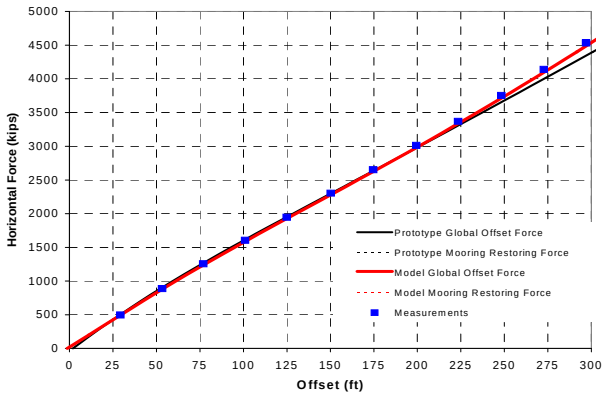

Fig.14 Horizontal Offset Curve

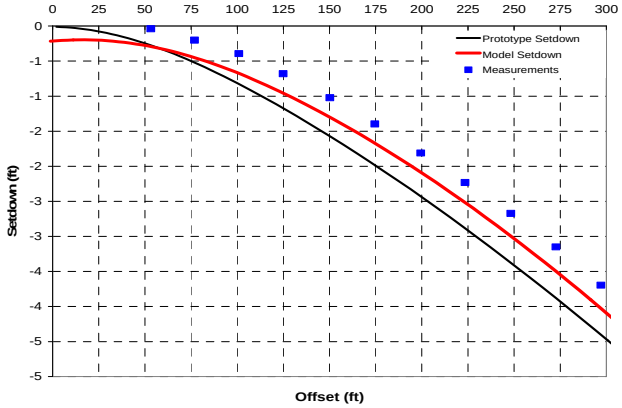

Fig.15 Vertical Setdown Curve

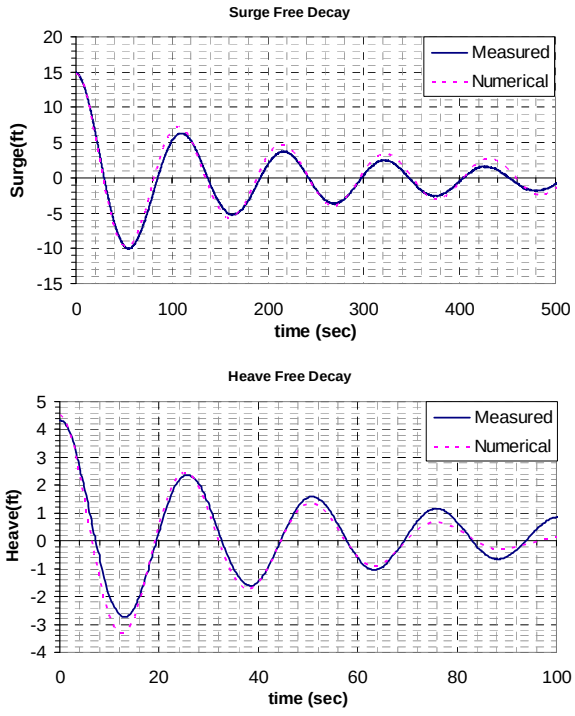

Fig.16 Free Decay Test of Surge and Heave

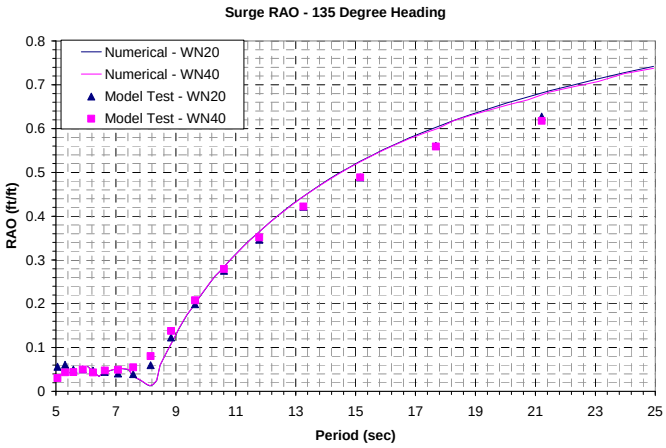

Fig.17 Surge RAO by a White Noise Test – 135 Degree

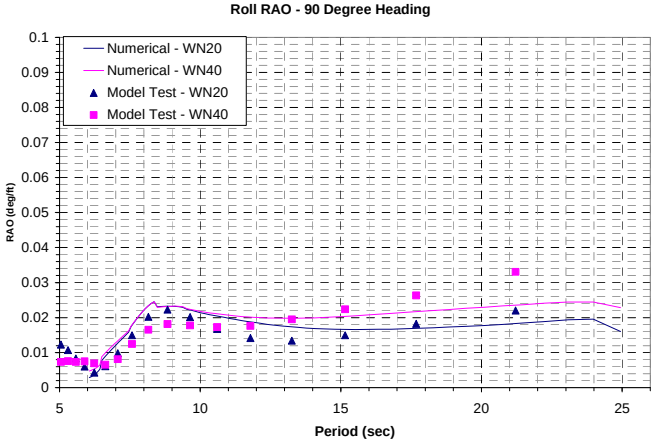

Fig.18 Roll RAO by a White Noise Test – 90 Degree Heading

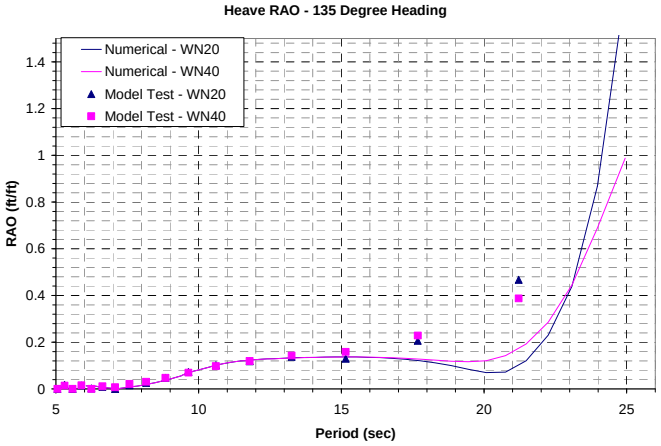

Fig.19 Heave Motion RAO by a White Noise Test – 135 Degree

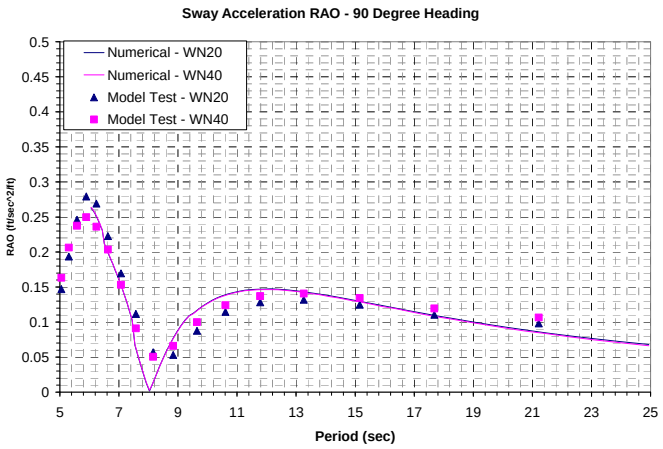

Fig.20 Horizontal Deck Acceleration RAO @ Deck Center – 90 Degree Heading

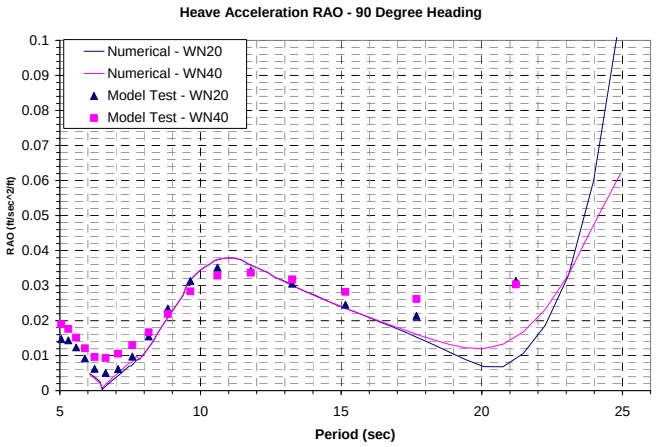

Fig.21 Vertical Deck Acceleration RAO at the Deck Center - 90 Degree Heading

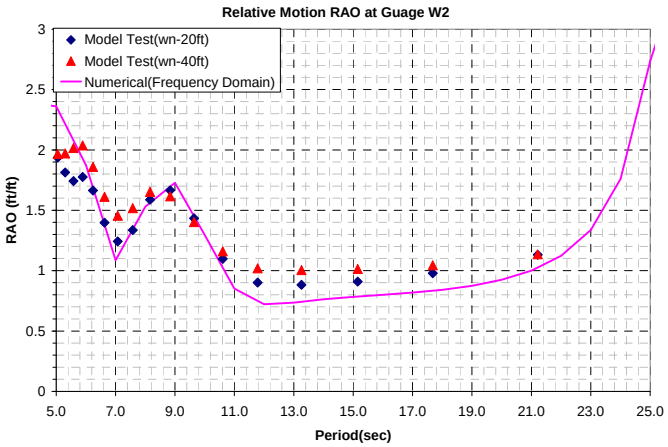

Fig.22 Relative Motion RAO for 90 Degree Heading at the Up-wave Column Front

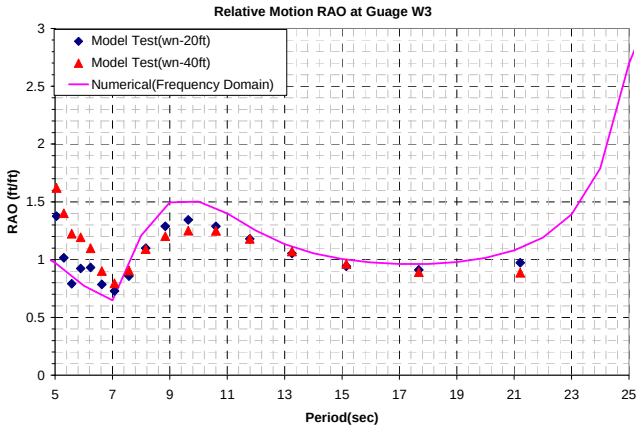

Fig.23 Relative Motion RAO for 135 Degree Heading at the Down-wave Column Front

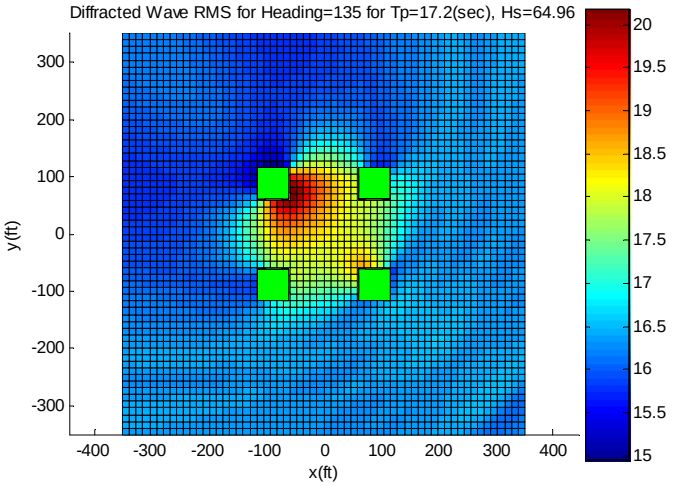

Fig.24 Simulated Wave RMS of Diffracted Wave Field around the Truss Semi – 1000 Year Hurricane Wave Dominant at 135 Degree Heading

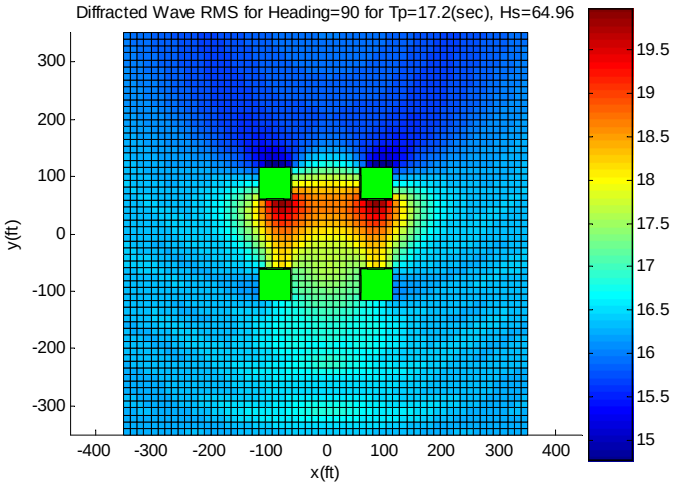

Fig.25 Simulated Wave RMS of Diffracted Wave Field around the Truss Semi – 1000 Year Hurricane Wave Dominant at 90 Degree Heading

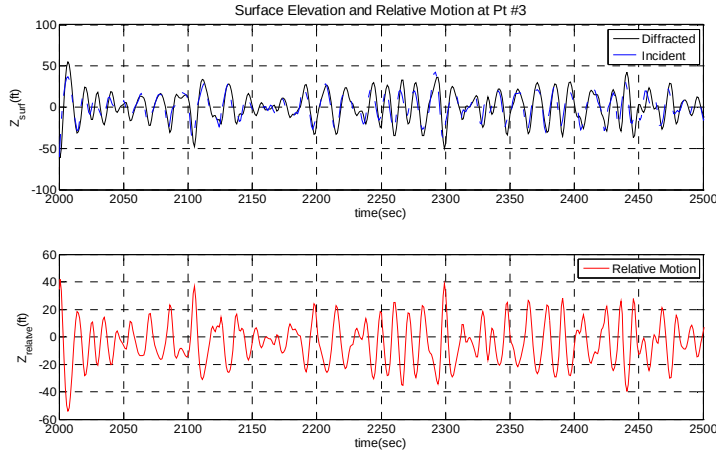

Fig.26 Incident Wave, Diffracted Wave and Relative Motion at the Down-wave Column Front – 135 Degree for 1000 year Hurricane Wave Dominant

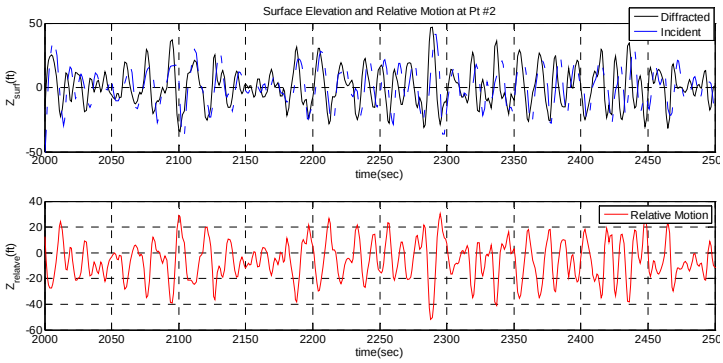

Fig.27 Incident Wave, Diffracted Wave and Relative Motion at the Up-wave Column Front – 90 Degree for 1000 year Hurricane Wave Dominant

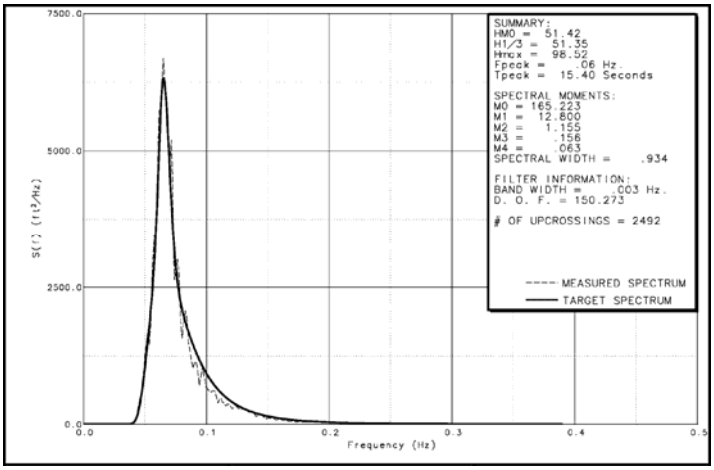

Fig.28 Wave Target and Measure Spectrum Matched – 100 Year Hurricane Wave Dominant

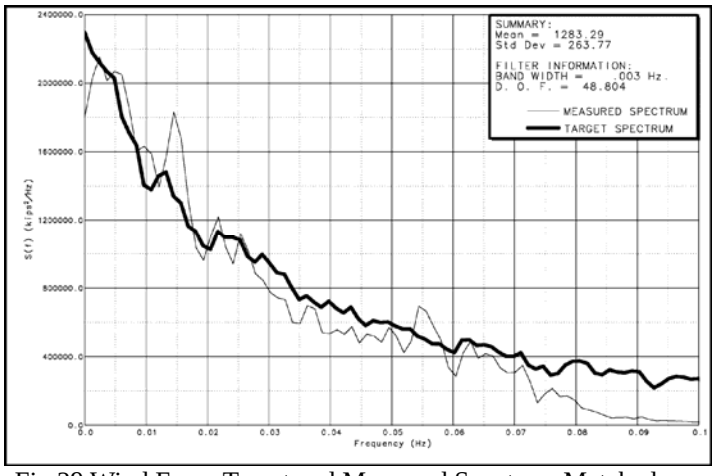

Fig.29 Wind Force Target and Measured Spectrum Matched – 100 Hurricane Wind Dominant

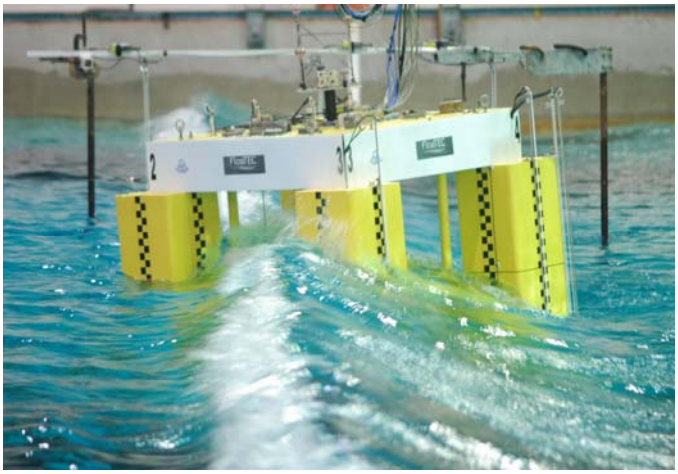

Fig.30 A Snapshot of 100 Year Hurricane Condition with 135 Degree Heading Angle

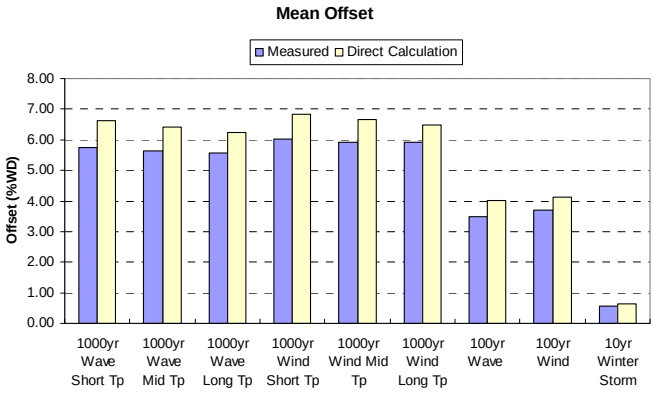

Fig.31 Mean Offset

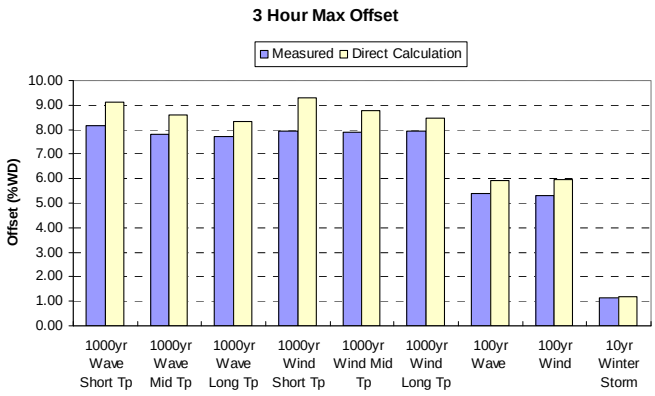

Fig.32 Three Hour Maximum Offset

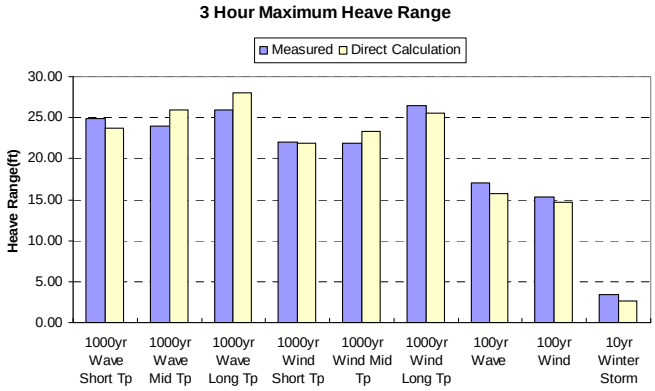

Fig.33 Three Hour Maximum Heave Range

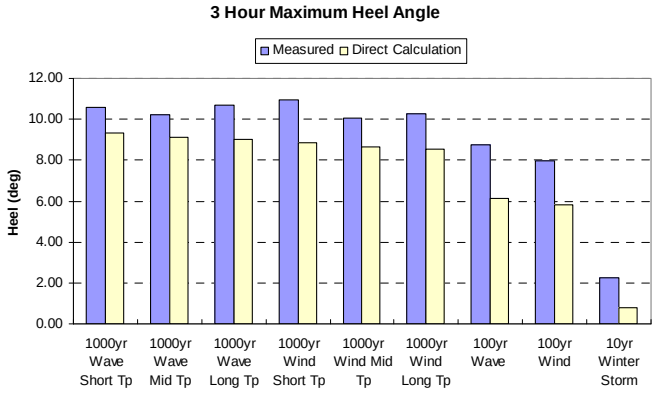

Fig.34 Three Hour Maximum Heel Angle

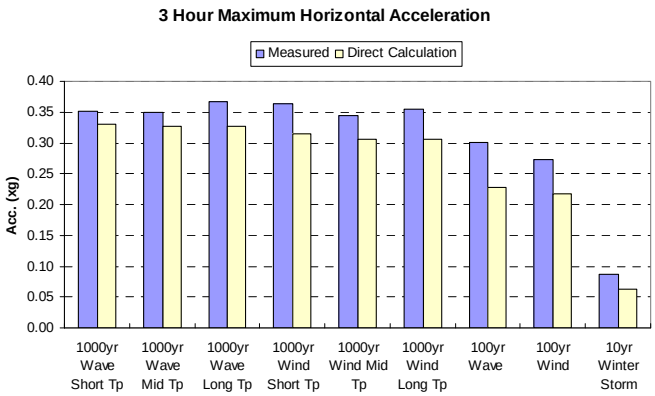

Fig.35 Three Hour Maximum Horizontal Acceleration @ Deck Center

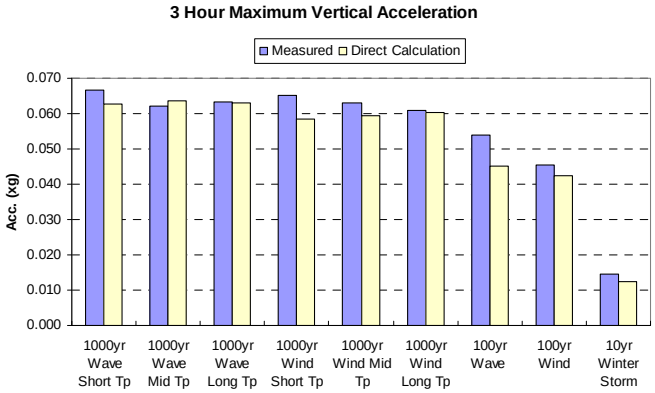

Fig.36 Three Hour Maximum Vertical Acceleration @ Deck Center

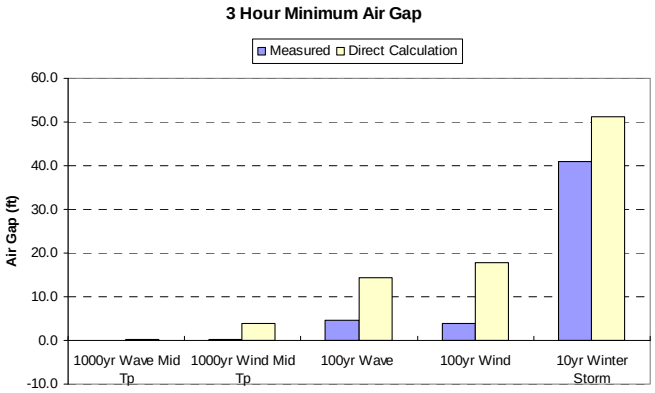

Fig.37 Three Hour Minimum Air Gap @ Bottom of Bottom Deck Steel for the Design Cases Only

Table 1 Payload for the Design of the Truss Semi

Parameter	
Water Depth (ft)	4,300
Region	GoM Atwater Valley
Production Rates	Oil 50,000 b/d Gas 50 Million scf/d
Risers	8 – TTR's Single Casing 1 – Drilling 2 – Gas/Oil Export SCRs
Number of Wells	8
Operating Workover Rig* (st)	7,997
Total Operating Topsides Weight* (st)	17,718.5
TTR Tensions (st) Production Risers	2000
TTR Tensions (st) Drilling Risers	450
SCR Vertical Load** (st)	702
Total Payload (st)	20,871

Table 2 Mooring Line Configuration

	Platform Chain	Rope	Ground Chain
Type	R4 Studless	Polyester	R4 Studless
Length(ft)	400.02	5905.8	250.01
Wet Weight(lbs/ft)	152.46	8.06	152.46
Dry Weight(lbs/ft)	175.31	21.9	175.31
EA or MBL (Kips)*	1.45E+05	2,750	2.08E+05
Diameter (in)	4.5	8.5	4.5
Ci	2	2	2
Cd	2.45	1.2	2.45

Table 3 Production Top Tensioned Riser Properties

Riser Type	Production (8)
OD (in)	10.75
WT (in)	0.6
Dry Weight Tolerance (%)	5
Material	API X-65
Length(ft)	4300
Wet Weight(lbs/ft)	52.01
Dry Weight(lbs/ft)	65.18
EA (Kips)	5.58E+05
EI (Kips-ft^2)	5.01E+04
# of Risers	8
Design Pressure (psi)	8645
Content Density(lbs/ft^3)	46.88
Top Pretension (Kips)	500
Tensioner Stiffness (Kips/ft)	14.3

Table 4 Drilling Riser Properties

Riser Type	Drilling (1)
OD (in)	16
WT (in)	0.75
Dry Weight Tolerance (%)	5
Material	API X-65
Length(ft)	4300
Wet Weight(lbs/ft)	95.68
Dry Weight(lbs/ft)	122.42
EA (Kips)	1.05E+06
EI (Kips-ft^2)	2.12E+05
# of Risers	1
Design Pressure (psi)	8645
Content Density(lbs/ft^3)	46.88
Top Pretension (Kips)	900
Tensioner Stiffness (Kips/ft)	25.7

Table 5 Principals of Truss Semi

Draft	(ft)	72
Freeboard	(ft)	75
Column Width	(ft)	55
Column Corner Radius	(ft)	5
Column CC Distance	(ft)	175
Pontoon Width	(ft)	35
Pontoon Corner Radius	(ft)	5
Pontoon Height	(ft)	25
Heave Plate Length (in-WE-dir)	(ft)	180
Heave Plate Width (in SN-dir)	(ft)	144
Heave Plate Draft	(ft)	-442
Truss Leg CC Distance	(ft)	108
Displacement	(Kips)	91,874.52
TTR Vertical Load	(Kips)	4,900.00
SCR Vertical Load	(Kips)	1,096.30
Mooring Vertical Load	(Kips)	3,739.12
Total Weight	(Kips)	82,139.10

Table 6 Environmental Criteria for the Model Test

		Gulf of Mexico Water Depth = 4300 ft				
Gulf of Mexico		1	2	3	4	5
Water Depth = 4300 ft		1000 year Hurricane		100 year Hurricane		**10 year Winter Storm**
		Wave Dominate	**Wind Dominate**	**Wave Dominate**	**Wind Dominate**	
		Survival Condition	Survival Condition	Design Extreme	Design Extreme	Operation Extreme
Wave		Jonswap	Jonswap	Jonswap	Jonswap	Jonswap
Gamma		2.20	2.20	2.20	2.20	2.20
Hs	(ft)	64.96	61.72	51.84	49.25	18.05
Tp	(s)	16.2 17.2 18.2	15.8 16.8 17.8	15.40	15.20	10.10
Hmax	(ft)	114.51	108.80	91.54	86.98	32.48
Cmax	(ft)	75.46	71.53	61.03	57.75	19.03
Surf. Current		7.38	7.38	5.91	5.91	1.64
Wind		**API**	**API**	**API**	**API**	**API**
1 hr @ 10m	(ft/s)	187.02	196.86	149.61	157.49	65.29
Direction	(deg)	90,135	90, 135	90, 135	90, 135	90, 135

Table 7 Wind Area and Center of Pressure of Topside

Heading	Wind Area(ft^2)	CP from MWL
135	43,050	84.4
90	37,435	84.4

Table 8 Current Load and the Center of Pressure

Heading	135 deg		90 deg	
Condition	Horizontal Force (Kips)	CP (ft, from MWL)	Horizontal Force (kips)	CP (ft, from MWL)
1000yr Wave	1,392.22	-58.2	1,469	-58.84
1000yr Wind	1,392.51	-58.17	1,469	-58.82
100yr Wave	807.09	-49.89	852	-50.72
100yr Wind	807.23	-49.87	852	-50.71
10yr Winter Storm	59.77	-50.11	63	-50.96

Table 9 Natural Period Measured and Calculated

	Measured		Numerical		Error
	Tn (sec)	Damping(%)	Tn (sec)	Damping(%)	(%)
Surge	106.5	6.9	108	6.30%	-1.39
Sway	108.5	9.9	106.5	10.40%	1.88
Heave	24.9	5.6	25.7	6.70%	-3.05
Roll	38.7	16.1	37.8	10.10%	2.26
Pitch	38	15.3	35.6	16.80%	6.61
Yaw	53.9	4.1	61.1	1.20%	-11.75